Molecular Crystals and Liquid Crystals

Publication details, including instructions for authors and subscription information:
http://www.tandfonline.com/loi/gmcl20

Selective Diffraction Reflection in Helical Periodical Media with Large Anisotropy

A. H. Gevorgyan [a] , M. Z. Harutyunyan [a] , A. Kocharian [b] & G. A. Vardanyan [c]

[a] Yerevan State University, Manookian, Yerevan, Armenia

[b] California State University, Northridge, CA, USA

[c] Intercontinental State University, C/O PACE, Los Angeles, CA, USA

Version of record first published: 31 Aug 2006

To cite this article: A. H. Gevorgyan, M. Z. Harutyunyan, A. Kocharian & G. A. Vardanyan (2005): Selective Diffraction Reflection in Helical Periodical Media with Large Anisotropy, Molecular Crystals and Liquid Crystals, 432:1, 69-82

To link to this article: http://dx.doi.org/10.1080/154214090960153

Mol. Cryst. Liq. Cryst., Vol. 432, pp. 69–82, 2005

ISSN: 1542-1406 print/1563-5287 online
DOI: 10.1080/154214090960153

Taylor & Francis
Taylor & Francis Group

Selective Diffraction Reflection in Helical Periodical Media with Large Anisotropy

A. H. Gevorgyan
M. Z. Harutyunyan
Yerevan State University, Manookian, Yerevan, Armenia

A. Kocharian
California State University, Northridge, CA, USA

G. A. Vardanyan
Intercontinental State University, C/O PACE, Los Angeles, CA, USA

Transmission and reflection of the light in films with helical periodical structure and enormous anisotropy are studied. We found strong evidence that in MgF_2 there is a range (window) of frequencies for the incident light where strong anisotropy takes place. It is shown that in helical periodical media (HPM) with large anisotropy, the circular dichroism in diffraction (selective) reflection region (DRR) decreases with the increasing of the parameter of anisotropy $\delta = (\varepsilon_1 - \varepsilon_2)/(\varepsilon_1 + \varepsilon_2)$ (where ε_1 and ε_2 are the principal values of the local dielectric constant tensor) and vanishes in the limit $\delta \gg 1$. The linear dichroism has the reverse behavior: it is equal to zero in the limit $\delta \ll 1$ and increases to the maximum value equal to one in the limit $\delta \gg 1$. The DRR's structures were also found at certain conditions for HPM calculated in the presence of dispersion for the dielectric permittivity.

Keywords: diffraction; eigen polarizations; large anisotropy; liquid crystals; selective reflection; transmission

INTRODUCTION

Optical properties of the HPM [cholesteric liquid crystals (CLC), chiral smectic liquid crystals, chiral sculptured thin films, magnetic helicoidal crystals, etc.] have extensively been studied both theoretically

The authors thank the unknown reviewer for valuable remarks and helpful recommendations.

Address correspondence to G. A. Vardanyan, Intercontinental State University, C/O PACE, 360 South Alameda St., Los Angeles, CA 90013, USA. E-mail: gagik2003@cs.com

and experimentally [1–6]. However, these discussions are usually limited to the case of the weak parameter of the anisotropy ($\delta \ll 1$). On the other hand, the recent technological progress in structuring multilayer systems with given parameters allows us to assume that there is a real possibility to synthesize and fabricate multilayer periodical systems of helical structure, for instance, using the media MgF_2 or TiO_2 with such values of local anisotropy δ, which varies greatly. For instance, it is well known that helical periodical media appear in nature and also can be synthesized as self-organized CLC [7] or fabricated by a variety of techniques, for example, by glancing-angle deposition on a rotating substrate [8]. There exist CLC polymer networks [9,10], too. CLC elastomers allow for mechanical tuning of the Bragg reflection region [9,11,12] because of the coupling of the polymer network and cholesteric structure.

An analogous situation (that is when $\delta > 1$) is expected for the artificial ferromagnetic helical structures imitating the behavior of CLC in the super-high frequency region, because, as is known, the magnetized ferromagnetics have large (enormous) anisotropy in the region of super-high frequencies near to ferromagnetic resonance [13,14].

All these make it urgent to develop the theory of transmission and reflection of light in the HPM with large anisotropy. Such investigations were started by Vardanyan *et al*. [15]. The investigation of the optical properties of HPM in artificially finely chirally sculptured MgF_2 or TiO_2 (in some ways, for instance, by glancing-angle deposition on a rotating substrate method or simply by uniform mechanical twisting of the rod form sample of MgF_2 or TiO_2) with relatively large ($\delta \sim 1$) and huge ($\delta \gg 1$) anisotropy is also of great interest because of many practical applications. We study the optical reflection in HPM with large anisotropy in this article.

The various characteristics of HPMs have recently become very important for optical applications [16–25]. Taking into account the experimental data from Refs. 26–28, the authors of those articles obtained the following dispersion relations of dielectric permittivity for the film media of MgF_2 and TiO_2:

$$\varepsilon'_x = \varepsilon^x_\infty + \sum_{i=1}^{3} 4\pi\rho_{ix}\omega^2_{Ti}\frac{\omega^2_{Ti} - \omega^2}{\left(\omega^2_{Ti} - \omega^2\right)^2 + \gamma_i^2\omega^2},$$

$$\varepsilon''_x = \sum_{i=1}^{3} 4\pi\rho_{ix}\omega^2_{Ti}\frac{\gamma_i\omega}{\left(\omega^2_{Ti} - \omega^2\right)^2 + \gamma_i^2\omega^2},$$

$$\varepsilon'_y = \varepsilon^y_\infty + 4\pi\rho_y\omega_T^2 \frac{\omega_T^2 - \omega^2}{\left(\omega_T^2 - \omega^2\right)^2 + \gamma^2 + \omega^2}, \quad (1)$$

and

$$\varepsilon'' = 4\pi\rho_y\omega_T^2 \frac{\gamma\omega}{\left(\omega_T^2 - \omega^2\right)^2 + \gamma^2 + \omega^2}.$$

The constants $4\pi\rho$ (oscillator strength), ω_T (transverse optical phonon frequency), γ/ω_T (γ is the line-width of the resonance), and ε_∞ (super-high frequency dielectric permittivity) were defined experimentally [26–28]. In Figure 1, the calculated dependences for (1) versus λ are shown for MgF_2. As it can be seen from Figure 1, there are some wavelength regions where $\varepsilon'_x(\lambda) > 0$ and $\varepsilon'_y(\lambda) > 0$, and vice versa. Thus, if $\lambda = 23.8\,\mu m$, then $\varepsilon'_x(\lambda) = 2.667$, $\varepsilon'_y(\lambda) = -2.638$, and $\delta = 182.93$; that is, these simulations show evidence that in MgF_2 there is a range of wavelengths for the light where strong anisotropy ($\delta \gg 1$) is expected.

OPTICAL PROPERTIES OF HPM LAYER WITH LARGE ANISOTROPY

For simplicity, we first consider the HPM optics with large anisotropy without taking into account the dielectric permittivity dispersion, although later we correctly take into account the dispersion and

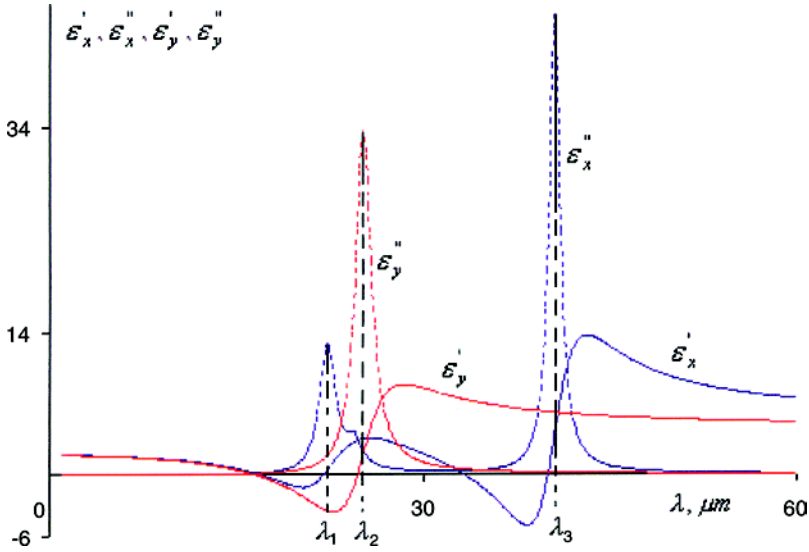

FIGURE 1 Dependences of $\varepsilon_x(\lambda)$, $\varepsilon'_y(\lambda), \varepsilon''_x(\lambda)$, and $\varepsilon''_y(\lambda)$ onto λ for MGF_2.

absorption. This is more convenient, because it allows us to find the main peculiarities related to the larger values of anisotropy and select the regions where $\delta \sim 1$ or $\delta \gg 1$. Also, it is easier to analyze the influence of dispersion and absorption on the various optical properties later.

Let us consider light propagation in an HPM along its helix axis. The dielectric permittivity, $\hat{\varepsilon}$, and magnetic permeability, $\hat{\mu}$, tensors have the form

$$\hat{\varepsilon}(z) = \varepsilon_m \begin{pmatrix} 1+\delta\cos 2az & \pm\delta\sin 2az & 0 \\ \pm\delta\sin 2az & 1-\delta\cos 2az & 0 \\ 0 & 0 & 1-\delta \end{pmatrix} \hat{\mu}(z) = \hat{I}. \qquad (2)$$

Here, $a = 2\pi/\sigma$, σ is the helix pitch, $\varepsilon_m = (\varepsilon_1 + \varepsilon_2)/2$, and $\hat{I}$ is the unit matrix. In this case, as is known, the field in the medium has the form brought in Ref. 4:

$$\vec{E}(z,t) = \sum_{j=1}^{4} [E_j^+ \vec{n}_+ \exp(ik_j^+ z) + E_j^{\rightarrow} \vec{n}_- \exp(ik_j^{\rightarrow} z)] \exp(-i\omega t), \quad j = 1,2,.,4 \qquad (3)$$

where $\vec{n}_\pm = (\vec{x} \pm i\vec{y})/\sqrt{2}$ are the circular polarization unit vectors and k_j^+ and k_j^- are the wave vectors' z components ($k_j^+ - k_j^- = 2a$). They are found from the dispersion equation and have the form

$$k_j^+ = 2\pi\sqrt{\varepsilon_m}(\chi \pm b^\pm)/\lambda, \; k_j^- = 2\pi\sqrt{\varepsilon_m}(-\chi \pm b^\pm)/\lambda. \qquad (4)$$

Here, $\chi = \lambda/(\alpha\sqrt{\varepsilon_m})$, λ is the wavelength in vacuum, $b^\pm = \sqrt{1+\chi^2 \pm \eta}$, and $\eta = \sqrt{4\chi^2 + \delta^2}$. The wave numbers $K_j = 2\pi b^\pm \sqrt{\varepsilon_m}/\lambda$ ($j = 1,2$), in the system of coordinates rotating with the director, are real quantities (in absence of absorption), except for DRR where the resonance wave number K_2 becomes purely imaginary. The equation $b^- = 0$ defines the boundaries of this region:

$$\lambda_{1,2} = \sigma\sqrt{\varepsilon_m(1 \pm \delta)}. \qquad (5)$$

At $\varepsilon_m > 0$ and $\delta < 1$, there is a finite DRR. At $\delta > 1$, the equation $b^- = 0$ has only one real solution, and this means that DRR begins at $\lambda = 0$ and reaches to $\lambda_1 = \sigma\sqrt{\varepsilon_m(1 \pm \delta)}$.

In the case of $\varepsilon_m < 0$ (also assuming that one of the principal values of the dielectric tensor is positive and $\delta > 1$ everywhere), one more characteristic wavelength (frequency) $\lambda_0 = \sigma|\delta|\sqrt{|\varepsilon_m|}/2$ appears defined by the condition $\eta = 0$. At wavelengths $\lambda > \lambda_0$, the quantity η

becomes purely imaginary and, therefore, wave numbers $k_j^{\pm}$ become complex. The equation $b^- = 0$, which determines the DRR boundaries, has only one solution, which is $\lambda_2 = \sigma\sqrt{\varepsilon_m(1-\delta)}$, where $\lambda_2 < \lambda_0$. Thus, the light interaction with the medium has a diffraction character in the range $0 < \lambda < \lambda_2$. The range $\lambda_2 < \lambda < \lambda_0$ defines the transmission region. At $\lambda > \lambda_0$, all the wave numbers are complex; therefore in this region the reflection has a nondiffraction character. It has mirror character and there is a finite region of transmission between the diffraction and mirror reflection regions.

Now let us consider the light transmission and reflection at its normal incidence (the incidence angle is zero) on a planer layer of HPM. The analytical solution of this boundary problem is known [1–5,29], and using those results we immediately pass to the discussion of the obtained results.

In Figure 2, the coefficient if reflection R is shown depending on wavelength λ, in the case of $\varepsilon_m > 0$ and $\delta \leq 1$, when circular polarized light is falling on HPM layer. The polarization coincides with the helix

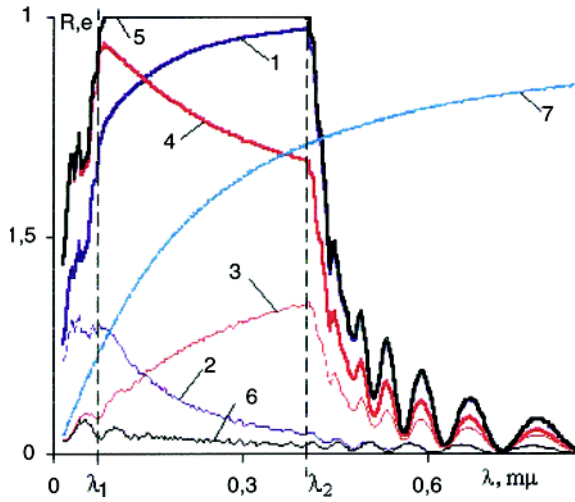

FIGURE 2 Dependence of the reflection coefficient R on the wavelength λ for the incident light, which has the right (1) and the left (2) circular polarizations; the linear polarizations along the direction of director at the entrance surface of HPM layer (3) and along the perpendicular direction (4); and the diffract (5) and opposite (6) EPs. Curve 7 presents the dependence of EP ellipticity onto λ (ellipticity of the second EP has the opposite sign). HPM is assumed to be right-handed. $\mathrm{Re}\varepsilon_\mathrm{m} = 0.5$, $\mathrm{Re}\delta = 0.95$, $\mathrm{Im}\varepsilon_\mathrm{m} = 0$, $\mathrm{Im}\delta = 0$. $\sigma = 0.42\,\mathrm{m}\mu$, and $d = 7\sigma$. Reflection from the HPM layer is considered.

screw ("a resonance circular polarization," curve 1); the same is also shown for the reverse circular polarization ("nonresonance circular polarization," curve 2). Those dependences for both linear polarizations are also shown (curves 3 and 4). The case of $\varepsilon = \varepsilon_m$ (where ε is the dielectric permitivity of the medium, which has boundaries on both sides of HPM layer) is considered to minimize the dielectric boundary influence. As it is seen from Figure 2 in the DRR region $\lambda_1 < \lambda < \lambda_2$, the reflection R sharply differs from zero for the both circular polarizations of the falling light, whereas at $\delta \ll 1$ the circularly polarized light with the same handedness as the structure itself reflects diffractively ($R \sim 1$), while the light with opposite circular polarization is transmitted through the structure without any diffraction reflection (in DRR range the reflection coefficient practically vanishes). Therefore, DRR, in the case of HPM, often is called the region of selective diffraction reflection (for circular polarizations). Thus, for larger anisotropies, the complete diffraction selectivity (in the sense that the interaction of the light of one circular polarization with HPM layer has a diffraction nature, whereas the light with another circular polarization has no diffraction nature) for circular polarizations (which is one of the main characteristics of HPM) is lost, and now the interaction of light with media has a diffraction nature for the both circular polarizations. Let's note that the selectivity of reflection in HPM both for circular and linear polarizations is practically always present at any value of anisotropy; that is, the curves $R(\lambda)$ are sufficiently different for both circular and linear polarizations.

Notice that there is a strong diffraction reflection, if the layer is geometrically thin ($d \sim 1 \div 3\sigma$, d is HPM layer thickness), whereas at $\delta \ll 1$ it takes place at $d \sim 30 \div 50\sigma$. This is because diffraction efficacy for HPM depends not only on the layer thickness, but also on the parameter δ/σ (i.e., depends onto $d\ \delta/\sigma$), which is large in this case because of the large δ.

In Figure 3, the reflection coefficient R*'s* dependence on wavelength λ is represented when a transmission region ($\lambda_2 < \lambda < \lambda_0$) between diffraction ($0 < \lambda < \lambda_2$) and mirror ($\lambda_0 < \lambda < \infty$) reflection regions (in the case of $\varepsilon_m < 0$) are formed. The larger reflection within the transmission region is a Fresnel type and not diffraction one. Here the light reflection from the half-space is considered.

As the detailed investigations show, these peculiarities are due to Eigen polarization (EPs) changes connected with anisotropy changes. As is known, EPs are the two polarizations of incident light that remain unchanged when light passes through an optical system. In general, the ellipticities of EPs practically coincide with those of medium internal waves (eigenmodes). Of course, there are some

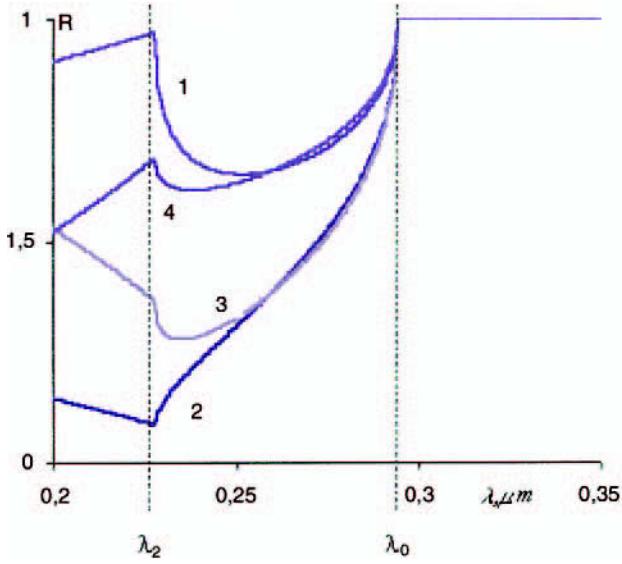

FIGURE 3 Dependence of the reflection coefficient R on the wavelength λ. Numbering of curves is the same as in Figure 2. HPM is assumed to be right-handed. $\mathrm{Re}\varepsilon_{\mathrm{m}} = 0.1$, $\mathrm{Re}\delta = 5.0$, $\mathrm{Im}\varepsilon_{\mathrm{m}} = 0$, $\mathrm{Im}\delta = 0$, $\sigma = 0.42\,\mathrm{m}\mu$, and $d = 7\sigma$. Reflection from the HPM half-space is considered.

differences between them. In EPs, the influence of dielectric boundaries is taken into account. There are only two EPs whereas the eigenmodes can be more than two and moreover can differ from each other, for instance, for nonreciprocal media.

Let us introduce a ratio of complex field components of the falling wave (expanded by basic circular polarizations) as $\beta_i = E_i^-/E_i^+$ and the same for the transmitted wave as $\beta_t = E_t^-/E_t^+$. Two EPs $\beta_{1,2}$ are obtained from condition $\beta_i = \beta_t$, and, for the case of light transmission through a finite HPM layer with $\varepsilon = \varepsilon_m$ and $ad = 2\pi n$ (n is integer), they have the form

$$\beta_{1,2} = \frac{2\chi \pm \eta}{\delta}. \tag{6}$$

(In the general case, these expressions are rather complicated.) It is seen from Eq. (6) that EPs are two quasi-circular left- and right-hand polarizations if the anisotropy is weak ($\delta \ll 1$). These EPs change with anisotropy, and if the latter increases they turn into elliptic polarizations. The further anisotropy increases brings to the decrease (modulo) and vanishing of ellipticity for $\delta \gg 1$. Thus, if at one limit ($\delta \ll 1$) EPs

are orthogonal quasi-circular polarizations, at the other limit ($\delta \gg 1$) they are orthogonal but have quasi-linear polarizations.

The HPM EPs have another important property. As was already mentioned, at weak anisotropy, the HPM layer shows diffraction selectivity in regard to the circular polarizations, in the sense that the interaction of the light one circular polarization with the HPM layer has a diffraction nature, whereas the light with another circular polarization has no diffraction nature. If the anisotropy is huge ($\delta \gg 1$), it exhibits diffraction selectivity in regard to the linear polarizations, in the sense that now the interaction of the light of one linear polarization with the HPM layer has a diffraction nature, whereas the light with another linear polarization does not have that nature. For the intermediate anisotropy values, HPM layers lose their full diffraction selectivity in regard to these polarizations, and the interaction of the light with media has a diffraction nature both for circular and linear polarizations. The EPs' property analysis shows that at normal incidence diffraction, selectivity is a general property of the HPM layer. It is to be noted that these media show diffraction selectivity not for circular or linear polarizations, but only in regard to EPs. The light with one given EP shows complete diffraction reflection, and the reflection coefficient in DRR precisely equals to the unit and is independent of anisotropy. The light with another EP does not undergo any diffraction reflection at all. The reason the medium shows diffraction selectivity in regard to circular polarizations at weak anisotropy is that at this limit EPs coincide with these polarizations. In the same way, at huge anisotropy, the HPM layer shows selectivity for linear polarizations, because at this limit the EPs turn into linear orthogonal polarizations.

In Figure 2, the reflection coefficient dependence on wavelength is shown for the light falling on the layer; it has a diffracting EP (curve 5) and a nondiffracting EP (curve 6). The EP ellipticity dependence on wavelength is also shown (curve 7).

Let's note that the fact that the internal waves of HPM have elliptical polarization is well known, but the influence of anisotropy on ellepticity of those waves has not been investigated. Analogical investigations of the influence of the incidence angle's changes on the polarizations of eigenmodes were carried out by Yuvaraj and Suresh [30]. Endo *et al*. [31] investigated the absorption peculiarities of oblique light incidence on the CLC layer found that absorption suppression is observed only for incident angles of less than 19°. Yuvaraj and Suresh [30] show that this is connected with those changes of the polarizations of the eigenmodes, which are due to the incident angle's changes [the polarizations of the eigenmodes

change from the circular polarizations (at normal incidence) to linear ones (at grazing)].

The circular dichroism $D_c = (T^+ - T^-)/(T^+ + T^-)$ and linear dichroism $D_L = (T^x - T^y)/(T^x + T^y)$ are often measured in the experiment; here T^+ and T^- are the transmission coefficients for "resonance" and "nonresonance" circular polarizations, and T^x and T^y are those for the lights linearly polarized along the direction of the director and polarized perpendicularly to the director, respectively. If anisotropy is weaker ($\delta \ll 1$), the HPM layer circular dichrosim in DRR is practically equal to the unit, and oscillating, it vanishes out of this region. If the anisotropy δ increases, then circular dichroism D_c decreases (in DRR) and vanishes at the limit $\delta \gg 1$. The HPM with weak anisotropy does not show any linear dichroism. The increase of the anisotropy δ brings to linear dichroism in DRR. Outside of DRR, it decreases oscillatingly.

So far in discussing the optical properties of HPM with huge anisotropy, we considered the permitivity tensor principal values to be constant, that is, independent of frequency, and we assumed the absorption to be weak. Such an assumption was made to represent the effects connected with large anisotropy in the simplest way. It is also natural to take permitivity dispersion into account.

Dispersion causes various effects [32–36, and some others cited therein]. More than one Bragg regime can exist because of dispersion [32–35]. We consider one special case at which the huge anisotropy effects shall also appear. Let us consider light reflection from the actual material layer, namely from the magnesium fluoride (MgF_2) layer artificially and uniformly sculptured (in some way) into a spiral, forming the finely structured HPM layer. Moreover, we assume that in this process its local dielectric properties do not change, and hence the principal values of the local dielectric-constant tensor of HPM layer are defined as $\varepsilon_1 = \varepsilon'_x + i\varepsilon''_x$, $\varepsilon_2 = \varepsilon'_y + i\varepsilon''_y$, where $\varepsilon'_x, \varepsilon''_x, \varepsilon'_y, \varepsilon''_y$ are defined by dispersion law (1).

Besides, we consider the more general case, $\varepsilon \neq \varepsilon_m$, because it is practically impossible to provide the condition $\varepsilon = \varepsilon_m$ at the dielectric permitivity frequency dispersion.

In Figure 4a, the reflection coefficient dependence on wavelength λ is shown when circular polarized light is falling on a HPM layer and the polarization coincides with helix screw (curve 1); the same is also shown for reverse circular polarization (curve 2); and dependences for both linear polarizations are also shown (curves 3 and 4). Here the light reflection from the half-space is considered.

As it is seen form Figure 1, there are three resonance absorption lines, near $\lambda_1 = 22.2\,\mu m$, $\lambda_2 = 25.1\,\mu m$, and $\lambda_3 = 40.5\,\mu m$. Figure 4a

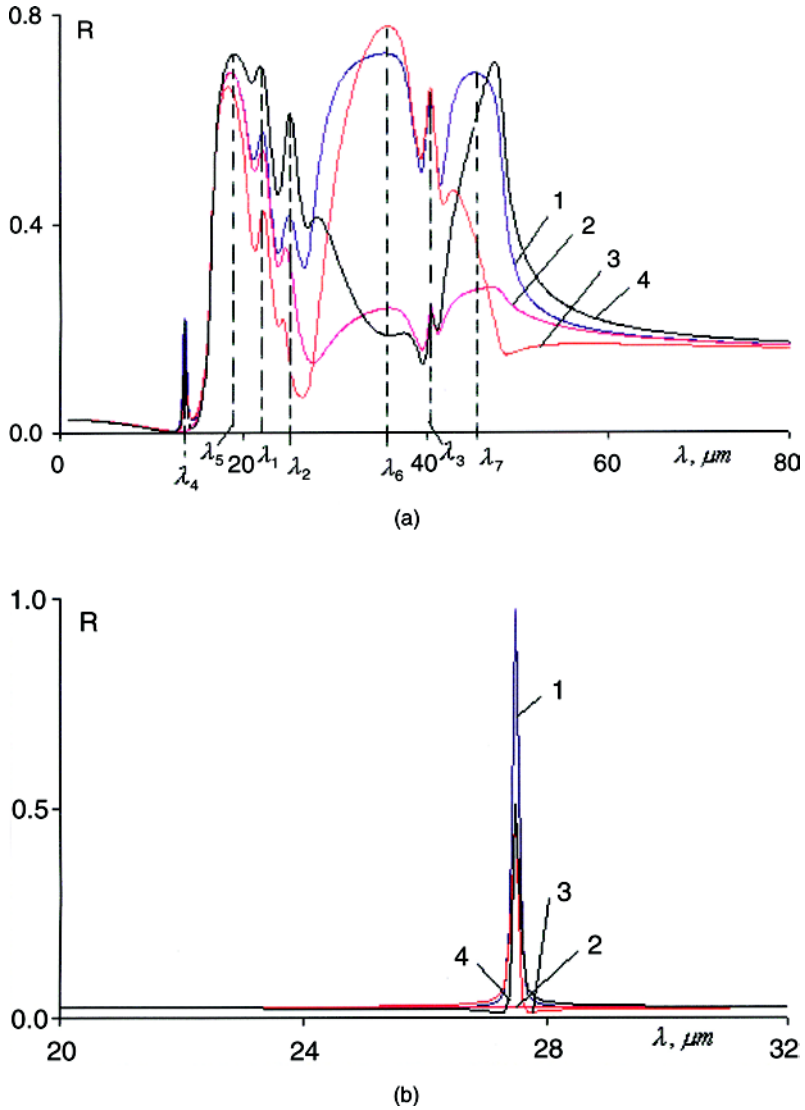

FIGURE 4 (a) Dependence of the reflection coefficient R on the wavelength λ in the presence of dispersion, with local dispersion low (1). $\varepsilon_x^\infty = 2.70$, $\varepsilon_y^\infty = 2.68$, $\sigma = 15\,\text{m}\mu$, $\varepsilon = 1$, $4\pi\rho_1 = 2.21$, $4\pi\rho_2 = 0.19$, $4\pi\rho_3 = 1.14$, $4\pi\rho = 2.70$, $\omega_{T1} = 247\text{cm}^{-1}$, $\omega_{T2} = 410\ \text{cm}^{-1}$, $\omega_{T2} = 450\,\text{cm}^{-1}$, and $\omega_T = 399\,\text{cm}^{-1}$. Numbering of curves is the same as in Figure 2. (b) Dependence of the reflection coefficient R on the wavelength λ, in the absence of dispersion.

shows the existence of reflection peaks near these lines. High reflection around these lines does not have a diffraction nature and is conditioned by the high values of imaginary parts of dielectric permitivities, and it is an analog of the high reflection from metallic surfaces. High reflection around the wavelenghts $\lambda_4, \lambda_5, \lambda_6$, and λ_7 (Figures 4a and 5) has a diffraction nature. For comparison, the dependence of $R(\lambda)$ at the absence of dispersion is presented in Figure 4b.

As is seen, the falling light with both circular polarizations undergoes a diffraction reflection, when there is dispersion. In this case, another interesting phenomenon appears. Figure 4a shows that in this case DRR breaks up into four DRRs. It is explained as follows (about the case of more than one DRR, see also Refs. 32–35).

Let us take the dimensionsless wave numbers $b^{\pm}$ in the form:

$$b^{\pm} = \sqrt{\left(\frac{b_1 + b_2 + 4\chi^2}{2}\right) \pm \sqrt{\left(\frac{b_1 + b_2 + 4\chi^2}{2}\right)^2 - b_1 b_2}}, \qquad (7)$$

where $b_{1,2} = 1 \pm d - c^2 \cdot b_1$ and b_2 have different signs in DRR; hence, b^- is purely imaginary here. Consequently, it can be asserted that DRR borders are the abscissas of intersections of points of the straights $y_1 = \sqrt{1-\delta}$ and $y_2 = \sqrt{1+\delta}$ with the straight $y = \chi$. If dispersion is

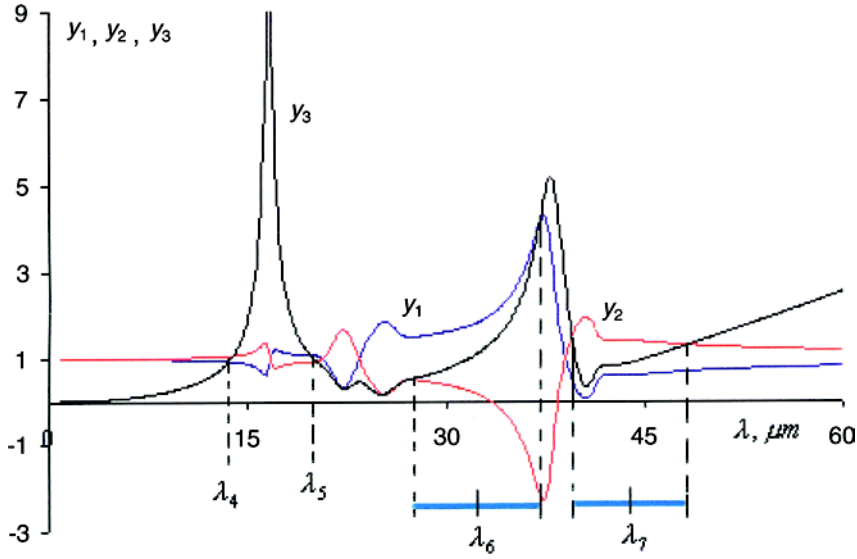

FIGURE 5 Dependences $y_1(\lambda)$, $y_2(\lambda)$, and $y_3(\lambda)$, in the presence of dispersion.

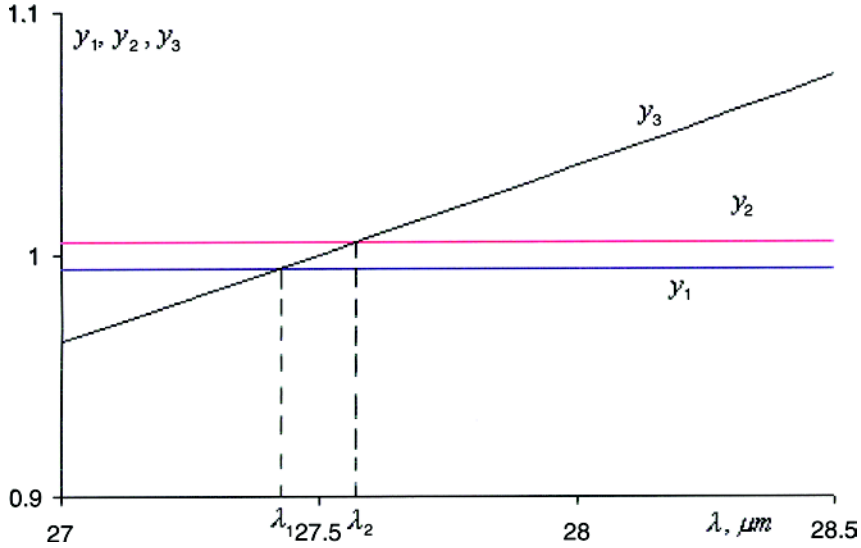

FIGURE 6 Dependences $y_1(\lambda)$, $y_2(\lambda)$, and $y_3(\lambda)$, in the absence of dispersion.

absent, there are two intersection points of $y = \chi$ with $y_1 = \sqrt{1-\delta}$ and $y_2 = \sqrt{1+\delta}$, and the abscissas of these points define DRR borders (λ_1 and λ_2, Figures 4b and 6. In the region of DRR, $y = \chi$ is above $y_1 = \sqrt{1-\delta}$ but below $y_2 = \sqrt{1+\delta}$. But, if there is dispersion, then both δ and ε_m become functions of wavelength λ, and the straight lines are replaced by complicated curves $y(\lambda) = \chi = \dfrac{\lambda}{\sigma\sqrt{\varepsilon_m(\lambda)}}$, $y_1(\lambda) = \sqrt{1-\delta(\lambda)}$, and $y_2(\lambda) = \sqrt{1+\delta(\lambda)}$, and consequently, depending on these functions, there can be several new DRRs (Fig. 5). In our case, new DRRs appear near λ_4, λ_5, λ_6, and λ_7 (Figs. 4a and 5).

Here, it is worth mentioning the influence of dispersion absorption. Generally, new DRRs do not arise in spectral regions of large absorption, even when $y(\lambda) = \chi$ is above $y_1(\lambda) = \sqrt{1-\delta(\lambda)}$ and below $y_2(\lambda) = \sqrt{1+\delta(\lambda)}$. Indeed, the intensity of diffraction reflection is characterized by the parameter $d\delta/\sigma$. The absorption effectively decreases this parameter and the diffraction reflection usually takes place when $d\delta/\sigma \sim 1$. But if absorption is strong, the medium absorbs the radiation at less penetration depth and the absorption saturation length is less than the diffraction saturation length.

In conclusion, we found that there is a large window of frequencies in MgF_2 where strong anisotropy must be observed. Moreover, the

DRRs structures are retained also in the presence of dispersion for the dielectric permitivity. The HPM has wide application, particularly as laser mirrors, display devices, polarization filters, modulators, and so forth mainly because of the Bragg diffraction phenomena in such media [16–25]. The represented results show that by varying the parameter of the anisotropy δ, we can change the DRR width (within large limits), and polarization of reflected and transmitted lights in DRR will give rise to mirror reflection regions and transparency windows between the mirror and diffraction reflection regions. Naturally, all these opportunities enlarge the possible limits and regions of application of HPM with large anisotropy. In conclusion, let us note that small geometrical thicknesses of HPM layers are important for designing miniature optical systems with large anisotropy.

REFERENCES

[1] De Vries, Hl. (1951). *Acta Cryst*., *4*, 219–226.
[2] Kats, A. I. (1970). *Zh. Eksp. Teor. Fiz*., *59*, 1854–1862.
[3] Nityananda, R. (1973). *Mol. Cryst. Liq. Cryst*., *21*, 315.
[4] Beljakov, V. A. (1992). *Diffraction Optics of Complex-Structured Periodic Media*, Springer-Verlag: New York.
[5] Chandrasekhar, S. (1977). *Liquid Crystals*., Cambridge: London.
[6] De Gennes, P. G. (1974). *The Physics of Liquid Crystals*., Oxford U. Press: London.
[7] Elston, S. & Sambles, R. (1998). In: *The Optics of Thermotropic Liquid Crystals*, Taylor and Francis: Bristol, PA.
[8] Robbie, K., Broer, D. J., & Brett, M. J. (1999). *Nature London*, *399*, 764.
[9] Finkelman, H., Kim, S. T., Muñoz, A., Palffy-Muhoray, P., & Taheri, B. (2001). *Adv. Mater*, *13*, 1069.
[10] Schmidtke, J., Stille, W., Finkelman, H., Kim, S. T., Muñoz, A., Palffy-Muhoray, P., & Taheri, B. (2002). *Adv. Mater*., *14*, 746.
[11] Bermel, P. A. & Warner, M. (2002). *Phys. Rev. E*, *65*, 056614.
[12] Cicuta, P., Tajbakhsh, A. R., & Terentjev, E. M. (2002). *Phys. Rev. E*, *65*, 051704.
[13] Raikher, Yu. A., Burilov, S. V., & Zakhlenikh, A. N. (1986). *Zh. Eksp. Teor. Fiz*., *91*, 542.
[14] Zvezdin, A. K. & Kotov, V. A. (1997). *Modern Magnetooptics and Magnetooptical Materials*, Institute of Physics Publishing: Bristol and Philadelphia.
[15] Vardanyan, G. A., Gevorgyan, A. H., Eritsyan, O. S., Arakelyan, O. M., & Tovmasyan, G. A. (1998). *Cryst. Rep*., *43*(5), 740–747.
[16] Venugopal, V. C. & Lakhtakia, A. (1998). *Opt. Commun*., *145*, 171–187.
[17] Sunal Paul, D., Lakhtakia, A., & Messier, R. (1998). *Opt. Commun*., *158*(1–6), 119–126.
[18] Lakhtakia, A. & Hodgkinson, I. J. (1999). *Opt. Commun*., *167*(1–6), 191–202.
[19] Lakhtakia, A. & McCall, M. (1999). *Opt. Commun*., *168*, (1–6), 457–465.
[20] McCall, M. & Lakhtakia, A. (2000). *J. Mod. Opt*., *47*(4), 743–755.
[21] Gevorgyan, A. H., Papoian, K. V., & Pikichian, O. V. (2000). *Opt. Spectrosc*., *88*, 586–593.
[22] Subacius, D., Shiyanovskii, S. V., Bos, Ph., & Lavrentovich, O. D. (1997). *Appl. Phys. Lett*., *71*, 3323–3325.

[23] Yang, Y.-C., Kee, C.-S., Kim, J.-E., & Park, H. Y. (1999). *Phys. Rev. E*, *60*, 6852.
[24] Schmidtke, J., Stille, W., & Finkelman, H. (2003). *Phys. Rev. Lett*., *90*, 083902.
[25] Kopp, V. I. & Genack, A. Z. (2002). *Phys. Rev. Lett*., *89*, 033901.
[26] Barker, A. S. (1964). *Phys. Rev*., *136*, 1290.
[27] Spitzer, W. G., Miller, R. C., Kleinman, D. A., & Howrath, L. E. (1962). *Phys. Rev.*, *126*, 1710.
[28] Briskin, V. V., Mirlin, D. N., & Reshina, I. I. (1973). *Sold State Physics (Russian FTT)*, *15*, 1118.
[29] Vardanyan, G. A. & Gevorgyan, A. H. (1997). *Cryst. Rep*., *42*(2), 276–279.
[30] Yuvaraj, Sah. & Suresh, K. A. (1994). *J. Opt. Soc. Am. A*, *11*(2), 740–744.
[31] Endo, S., Kuribara, T., & Akahane, T. (1983). *Jpn. J. Appl. Phys*., *22*, L499–L501.
[32] Gevorgyan, A. H. & Eritsyan, O. S. (1981). *Proc. Int. Conf. Soc. Cont. on Liq. Cryst*., Georgian SSR, Academy of Science Publication: Tbilisi, 409–410.
[33] Gevorgyan, A. H. (1983). *Izv. Acad. Sci. Arm. SSR, Fizika (Physical J. Acad. Sci. Arm SSR)*, *18*, 132–135.
[34] Wang, J., Lakhtakia, A., & Geddes III, J. B. (2002). *Optik*., *113*(5), 213–221.
[35] Lakhtakia, A. & Moyer, J. T. (2002). *Optik*., *113*(2), 97–99.
[36] Venugopal, V. C. (2000). *Eur. Phys. J.-Appl. Phys*., *10*, 173–184.